International Journal of Mechanics and Energy (IJME)
Vol. 1, Issue 3, 2013, ISSN: 2286-5845

Effects of magnetic field on Rayleigh-Bénard convection inside enclosures at different aspect ratios

Awatef NAFFOUTI*, Brahim BEN-BEYA, Taieb LILI
Laboratory of Mechanic of fluid, University of sciences of Tunis,
Department of physics, 2092 El Manar 2, Tunisia

Abstract: The present paper focuses, in particular, on aspect ratio (AR) effects on Rayleigh-Bénard convection within enclosure under a uniform magnetic field. Results are presented and analyzed for different values of Hartmann number ($60 \leq Ha \leq 80$) and for a range of aspect ratios ($0.75 \leq AR \leq 1$) at various Rayleigh numbers (Ra). It is found that both enclosure aspect ratio and magnetic field intensity play a significant role in controlling the onset of the Rayleigh-Bénard convection flow. The entropy generation analysis demonstrates that irreversibility phenomena increase for lower aspect ratio values and moderate Hartmann numbers.

Key words: Rayleigh-Bénard; Magnetoconvection; Entropy; Hartmann number.

1. Introduction

Natural convection in enclosures, in which heating from below and cooling from above, i.e. Rayleigh-Bénard convection (RBC), has long attracted considerable research interest in the literature[1-2].

The convection phenomenon that arises in fluid dynamics from the interaction of an electrically conducting fluid with the magnetic field is well known as magnetoconvection [3].

Magnetoconvection in cavities has become the basis of many scientific and engineering applications [4-5]. Numerous attempts have been made to analysis the Rayleigh-Bénard magnetoconvection (RBM) flow characteristics. Pirmohammadi et al. [6] conducted a steady, laminar, RBM flow in a tilted enclosure filled with liquid gallium. The authors revealed that as strength of the magnetic field is increased (Ha=70) convection is reduced and the heat transfer in the enclosure is mostly due to conduction mode.

Besides, numerous works on entropy generation, relating to natural and forced convection [7] demonstrate the importance of the topic.

*** Corresponding author:** Awatef NAFFOUTI
E-mail: awatef.naffouti@yahoo.fr.

2. Physical model

2.1. Rayleigh Bénard configuration

The physical model considered is shown in Fig. 1. It consists of a rectangular enclosure with height H and length L, leading to an aspect ratio (AR=L/H) filled with an electrically conducting fluid whose Prandtl number is 0.71. It is assumed that the vertical walls are adiabatic, while the horizontal walls are maintained at constant temperatures. We also assume that the enclosure is permeated by a uniform and constant horizontal magnetic field.

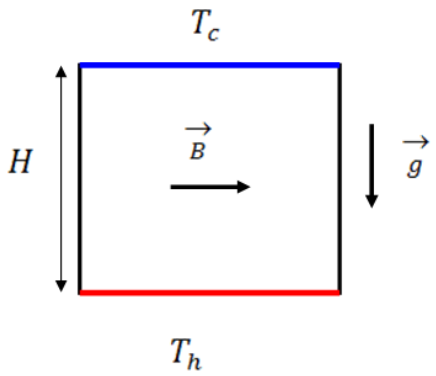

Fig.1. Physical model (Rayleigh-Bénard configuration).

2.2 Governing equations and boundary conditions

The governing equations which describe the system behavior are the mass continuity equation, the incompressible Navier–Stokes equations, and the energy conservation equation.

The dimensionless equations can be written as:

$$\frac{\partial u}{\partial x}+\frac{\partial v}{\partial y}=0$$

$$\frac{\partial u}{\partial t}+u\frac{\partial u}{\partial x}+v\frac{\partial u}{\partial y}=-\frac{\partial p}{\partial x}+\Pr\left(\frac{\partial^2 u}{\partial x^2}+\frac{\partial^2 u}{\partial y^2}\right)$$

$$\frac{\partial v}{\partial t}+u\frac{\partial v}{\partial x}+v\frac{\partial v}{\partial y}=-\frac{\partial p}{\partial y}+\Pr\left(\frac{\partial^2 v}{\partial x^2}+\frac{\partial^2 v}{\partial y^2}\right)+Ra\,\Pr\theta-\Pr Ha^2 v$$

$$\frac{\partial \theta}{\partial t}+u\frac{\partial \theta}{\partial x}+v\frac{\partial \theta}{\partial y}=\left(\frac{\partial^2 \theta}{\partial x^2}+\frac{\partial^2 \theta}{\partial y^2}\right)$$

with the boundary conditions:

$$u=v=0$$

$$\theta(x,0)=1;\ \theta(x,1)=0 \ \text{ at } \ 0\le x\le AR$$

$$\left.\frac{\partial \theta}{\partial x}\right|_{x=0}=\left.\frac{\partial \theta}{\partial y}\right|_{x=AR}=0 \qquad \text{at } \ 0\le y\le 1$$

From the above equations it is observed that the present problem is mainly governed by two parameters, namely the thermal Rayleigh number Ra and Hartmann number Ha, defined as follows:

$$Ra=\frac{g\beta\Delta TH^3}{\alpha\nu} \quad ; \quad Ha=BH\sqrt{\frac{\sigma}{\rho\nu}}$$

2.3 Entropy generation

Entropy generation in the cavity is due to two factors: heat transfer irreversibility and fluid friction irreversibility. Due to the existence of rather severe temperature gradients near and especially at the top corners of the heat source, the significant local entropy generation occurs close to these areas. Entropy generation is due to non-equilibrium flow imposed by boundary conditions through the channel walls.

The dimensionless local total entropy generation number (S), given by the local thermodynamic equilibrium of the linear transport theory, can be written as:

$$S=\left(\left(\frac{\partial T}{\partial x}\right)^2+\left(\frac{\partial T}{\partial y}\right)^2\right)+\varphi\left(2\left(\frac{\partial u}{\partial x}\right)^2+2\left(\frac{\partial v}{\partial y}\right)^2+\left(\frac{\partial u}{\partial y}+\frac{\partial v}{\partial x}\right)^2\right)$$

Dimensionless local entropy generation due to thermal gradients and that due to velocity gradients are given by:

$$STG=\left(\frac{\partial \theta}{\partial x}\right)^2+\left(\frac{\partial \theta}{\partial y}\right)^2$$

$$SVG=\varphi\left[2\left(\frac{\partial u}{\partial x}\right)^2+2\left(\frac{\partial v}{\partial y}\right)^2+\left(\frac{\partial u}{\partial y}+\frac{\partial v}{\partial x}\right)^2\right]$$

φ is the irreversibility coefficient given by:

$$\varphi=\frac{\mu T_0}{k}\left(\frac{\nu}{H\Delta T}\right)^2$$

which is taken constant at 0.1 in the present work.

From the above equation we have denoted the local entropy generation due to heat transfer by STG and the local entropy generation due to fluid friction by SVG.

3. Numerical approaches

Numerical solutions have been performed using a finite volume home code "NASIM" based on the projection method with the help of an accelerated multigrid solver. A projection method is used to couple the momentum and continuity equations. A finite-volume method is used to discredit the Navier–Stokes and energy equations. The advective terms are discredited using a QUICK third-order scheme. The Poisson pressure correction equation is solved using an accelerated multi-grid method [8].

In order to check the accuracy and reliability of the numerical procedure, Table 1 shows a comparison of calculated average Nusselt number (Nu) and the maximum stream function Ψ in the present work against the work of Ghasemi et al. [9] dealing with the magnetoconvection flow in differentially heated enclosure filled with nanofluid. It can be seen in Table 1 that the agreement is good, which indirectly validates the present computations and lend us confidence for the use of the suggested numerical model.

Table1 Comparison of our results with those of Ghasemi et al. [9] for Ra=10^5 and different Hartmann numbers.

Ha	Nu[9]	Nu	%	ψ_{max}[9]	ψ_{max}	%
0	4.738	4.7310	0.15	11.05	11.0469	0.050
30	3.150	3.1412	0.28	5.710	5.70798	0.035
60	1.851	1.8455	0.29	2.623	2.62125	0.067

4. Results

In this section the results of the numerical study are discussed in order to understand the natural convection of the flow in a square cavity in the presence of a magnetic field. Effects of applied magnetic field on the average Nusselt number and aspect ratio are discussed in detail.

The streamlines plot at Rayleigh number Ra in range $2\times10^5 \leq Ra \leq 5.5\times10^5$ gives a first overview of the general structure of the flow. Furthermore, for different Ra values, the influence of the Hartmann number and the aspect ratio on the flow patterns was investigated. We display in fig. 2 the evolution of streamlines with the Hartmann numbers. It can be pointed out that, for high aspect ratio number (AR=1), the flow patterns seems to be similar when the Hartmann number increases from 60 to 80. However, for small value of aspect ratio, the flow patterns changes noticeably, and one can observe an elongation of the eddies. As the Hartmann number increases, the Lorentz force effect increases. Consequently, the elongation of the eddies becomes more significant and its axis approaches the vertical. As can be noticed also in Fig.2 a rotating central cell occupies most of the cavity. Their intensities and their sizes increase as the Rayleigh number increases. The strength of circulation increases with a decreasing value of aspect ratio.

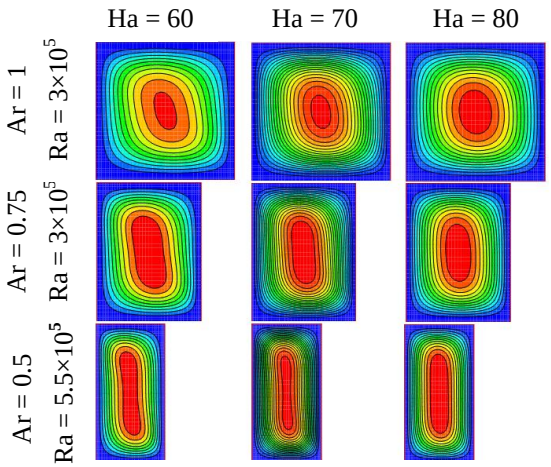

Fig.2. Streamlines for different AR and Ha numbers (Ha= 60, 70, and 80).

Fig. 3 shows the global kinetic energy magnitude over the whole cavity with three different AR and different Ha values. The predicted values using AR=0.5 are higher than those using AR=0.75 and 1. The simulated results is more remarkable at high Ha where vanishes and the deviation between the three aspect ratio is negligible, while it is more pronounced toward the first value Ha=60.

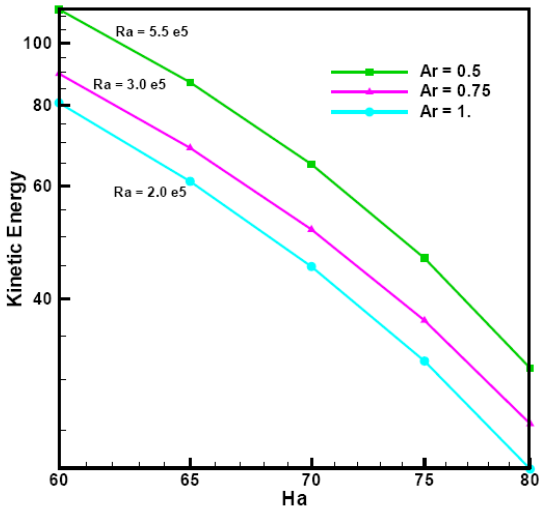

Fig .3. Variation of kinetic energy versus Hartmann number (Ha) at different aspect ratios (AR=0.5, 0.75, and 1).

In Fig.4 we report the total enstrophy of the flow named $\Omega(t)$ and defined as:

$$\Omega(t) = \frac{1}{2}\iint_D \omega^2(x, y, t)dxdy$$

where $\omega = \frac{\partial v}{\partial x} - \frac{\partial u}{\partial y}$ defines the dimensionless vorticity and (D) is the computed domain. Fig.4 displays the variation of the enstrophy for different aspect ratio and 50≤Ha≤80. The Ra is increased when AR decreases as reported in the same figure. The Ω remains weak when AR is in the vicinity of one, however, a significant decrease in Ω of the flow as a result of the attenuation of the flow by increasing Ha is observed.

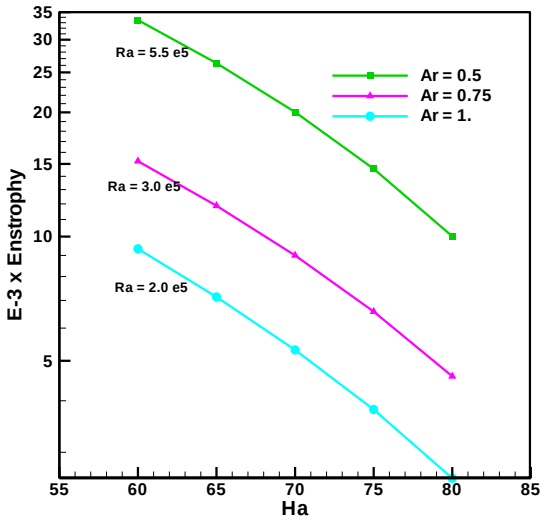

Fig. 4. Variation of Enstrophy versus Hartmann number (Ha) at different aspect ratio AR in range 0.5-1.

The flow structure revealed by isotherm plots in Fig.5 clearly indicates the distribution of temperature for $2\times10^5 \leq Ra \leq 5.5\times10^5$ at different values of aspect ratio ranging from 0.5 to 1. The intensity of convection is considerably decreased by the drag induced by the magnetic field, as indicated by a weak distortion of the isothermal lines. It's clearly seen that the large distortion of the isotherms is an indication of the decrease of the intensity of convection. Furthermore, Fig. 5 demonstrates that the increase of Hartmann number tends to slow down the movement of the fluid. This follow configuration is maintained up to Ha= 60, 70 and 80 for which the numerical results indicate that convection is suppressed by the magnetic field.

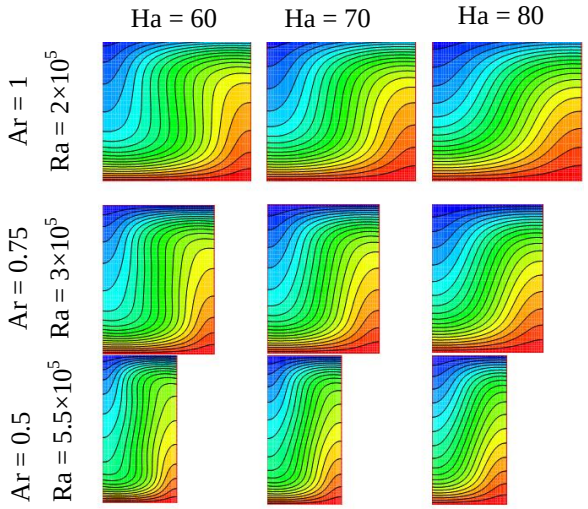

Fig.5. Isotherms at different AR and Ha numbers (Ha=60, 70, and 80).

The heat transfer rate across the fluid layer can be expressed in terms of the average Nusselt number at y=0 defined as:

$$\overline{Nu} = -\frac{1}{AR}\int_0^{AR}\left|\frac{\partial\theta}{\partial y}\right|_{y=0} dx$$

Fig.6 presents the variation of the average Nusselt number *Nu* versus Ha for different aspect ratios. From this figure, Nu increases considerably with the decrease of the aspect ratio because the circulation flow becomes stronger when the two vertical walls sufficiently approached. One can notice that in the absence of magnetic field (Ha=0), the heat transfer rate is relatively large than those obtained at high Ha values for which the flow currents vanish.

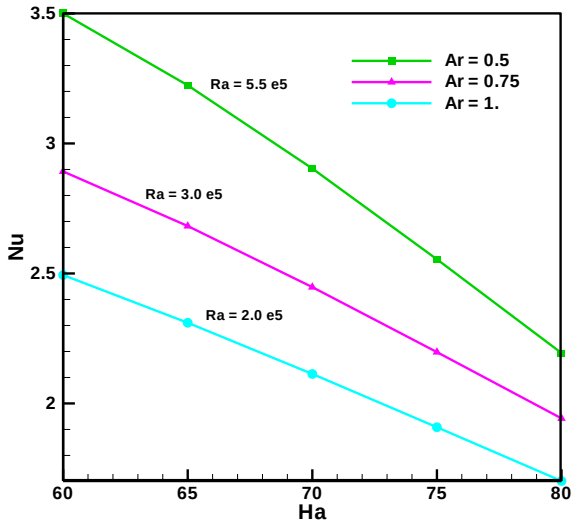

Fig.6. Variation of average Nusselt number versus Hartmann number (Ha), at different aspect ratios, AR in range 0.5-1.

For any aspect ratio, as seen in Fig.7, the heat transfer irreversibility (STG) is dominating for low Ha and higher for the case of square cavity (AR=1). The maps of local entropy generation corresponding to different aspect ratios and due to the heat transfer irreversibility are similar and decrease by increasing Ha as it is observed in Fig.7. This is mainly due to high temperature gradients manifested at high aspect ratio where the area of the heated wall from below is augmented.

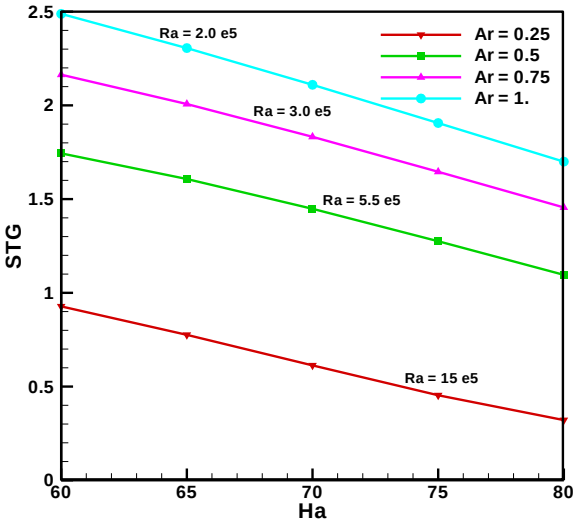

Fig.7. Irreversibility due to thermal gradient (STG) versus Hartmann number at different aspect ratios AR (0.25 to 1.).

5. Conclusion

In this paper the effects of aspect ratio on natural convection of Rayleigh-Bénard in an incompressible fluid in the presence of horizontal uniform magnetic field is analyzed and discussed.

The enstrophy of the flow remains weak for the square cavity (AR=1), however, a significant decrease in Ω is observed by increasing Ha. In the absence of magnetic field (Ha=0), the heat transfer rate is relatively larger than those obtained at high Ha values for which the flow currents vanish. The average Nusselt number Nu increases considerably with the decrease of the aspect ratio from 1 to 0.75. For the all investigated aspect ratios, the heat transfer irreversibility (STG) is dominating for low Hartmann numbers and higher for the case of square cavity.

References

[1] P.H. Kao, R.J. Yang, Simulating oscillatory flows in Rayleigh–Benard convection using the lattice Boltzmann method, International Journal of Heat and Mass Transfer 50 (2007) 3315–3328.

[2] M. Corcione, Effects of the thermal boundary conditions at the sidewalls upon natural convection in rectangular enclosures heated from below and cooled from above, International Journal of Thermal Sciences 42 (2003) 199–208.

[3] P. Kandaswamy, S.M. Sundari, N. Nithyadevi, Magnetoconvection in an enclosure with partially active vertical walls, Int. J. Heat Mass Transfer 51 (2008) 1946–1954.

[4] H. Ozoe, Magnetic Convection, Imperial College Press, 2005.

[5] N. Nithyadevi, P. Kandaswamy, S.M. Sundari, Magnetoconvection in a square cavity with partially active vertical walls: time periodic boundary condition, Int. J. Heat Mass Transfer 52 (2009) 1945–1953.

[6] M. Pirmohammadi, M. Ghassemi, Effect of magnetic field on convection heat transfer inside a tilted square

enclosure, International Communications in Heat and Mass Transfer 36 (2009) 776–780.

[7] I. Zahmatkesh, On the importance of thermal boundary conditions in heat transfer and entropy generation for natural convection inside a porous enclosure, Int J Thermal Sci 47 (2008) 339–346.

[8] N. Ben Cheikh, B. Ben Beya, and T. Lili, Benchmark solution for time-dependent natural convection flows with an accelerated full-multigrid method, numer. Heat Transfer B, vol. 52, (2007) 131–151.

[9] B. Ghasemi, S.M. Aminossadati, A. Raisi, Magnetic field effect on natural convection in a nanofluid-filled square enclosure, International Journal of Thermal Sciences 50 (2011) 1748-1756.